

## Supporting Information

### Amphiphilic drug-drug assembly via dual-responsive linkage for small-molecule anticancer drugs delivery

Tian Zhong <sup>1</sup>, Ran Huang <sup>2\*</sup>, Lianjiang Tan <sup>3\*</sup>

<sup>1</sup> Department of Chemistry and Pharmacy, Zhuhai College of Jilin University, Zhuhai 519041 Guangdong, China.

<sup>2</sup> State Key Laboratory of Microbial Metabolism and School of Life Sciences and Biotechnology, Shanghai Jiao Tong University, Shanghai 200240, China.

<sup>3</sup> Shanghai Center for Systems Biomedicine and Key Laboratory of Systems Biomedicine, Shanghai Jiao Tong University, Shanghai 200240, China.

\* Corresponding author. Tel: +86-21-34204561. E-mail: [ranhuang84@outlook.com](mailto:ranhuang84@outlook.com) and [litan@sjtu.edu.cn](mailto:litan@sjtu.edu.cn).

#### *Synthesis of AU1*

AU1 was synthesized according to the procedure reported in our previous work [1]. <sup>1</sup>H NMR (400 MHz, DMSO-d<sub>6</sub>): δ 9.99 (s, 2H, -NH(C=O)-), 8.06 (s, 1H, ArH), 7.84 (m, 2H, ArH), 7.31-7.23 (m, 24H, ArH), 7.20-7.15 (m, 6H, ArH), 2.26 (t, J = 7.2 Hz, 4H, -CH<sub>2</sub>S-), 2.10 (t, J = 7.1 Hz, 4H, -CH<sub>2</sub>CO-), 1.65-1.54 (m, 4H, -CH<sub>2</sub>CH<sub>2</sub>CH<sub>2</sub>-). ESI-MS m/z: calcd for C<sub>53</sub>H<sub>48</sub>N<sub>2</sub>O<sub>4</sub>S<sub>2</sub>Na, 863.2953; found, 863.2989 (M + Na<sup>+</sup>). The <sup>13</sup>C NMR spectrum was shown in Fig. S1.

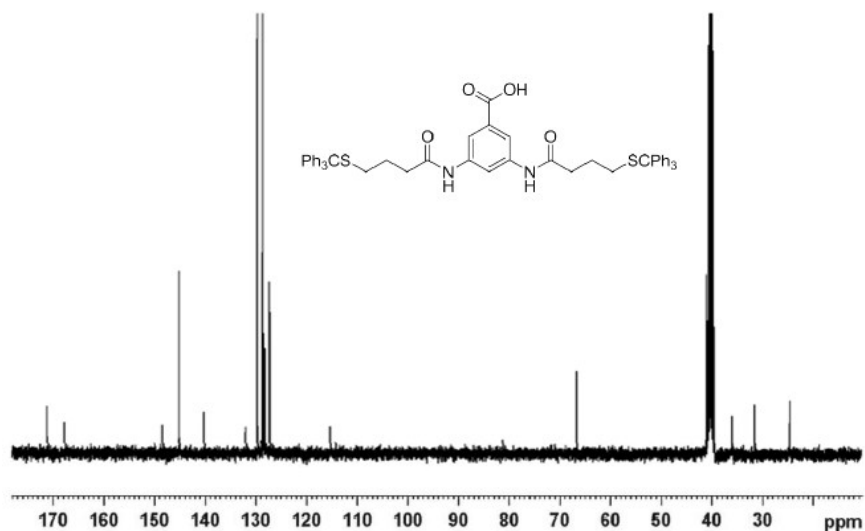
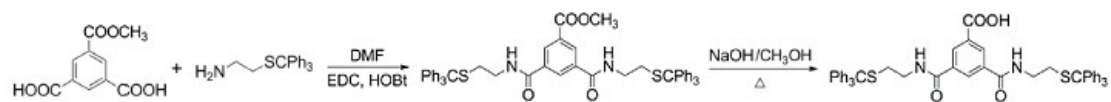


**Fig. S1.**  $^{13}\text{C}$  NMR spectrum of AU1 in  $\text{DMSO-}d_6$ .

#### *Synthesis of AU2*

The synthetic route of AU2 was illustrated in Scheme S1. To a stirred solution of trimesic acid monomethyl ester (2 mmol) and 2-(Tritylthio)ethanamine (6 mmol) in 20 mL of N,N-dimethylformamide (DMF), 1-ethyl-3-(3-dimethylaminopropyl)carbodiimide hydrochloride (EDCI, 4.8 mmol) and N-hydroxybenzotriazole (HOBt, 4.8 mmol) were added at 0 °C. After stirring for 4 h, 3 mL of sodium hydroxide solution (1 M) and 3 mL of methanol were added to the mixture, which was then heated to 50 °C and kept under stirring for 30 min. The resultant solution was poured into 40 mL of ice-water mixture, and the precipitate was filtered and distilled in vacuum to give AU2 with a yield of 57 %.  $^1\text{H}$  NMR ( $\text{CDCl}_3$ , 400 MHz)  $\delta$  7.78 (s, 1H, ArH), 7.43-7.34 (m, 12H, ArH), 7.30-7.14 (m, 19H, ArH), 7.06 (s, 2H, ArH), 6.35 (t,  $J = 5.6$  Hz, 2H,  $-\text{NHCH}_2-$ ), 3.27-3.19 (m, 4H,  $-\text{NCH}_2-$ ), 2.49 (t,  $J = 6.4$  Hz, 4H,  $-\text{SCH}_2-$ ), 1.45-1.41 (t,  $J = 15.2$  Hz, 3H,  $-\text{CH}_2-$ ). ESI-MS  $m/z$ : calcd for  $\text{C}_{51}\text{H}_{44}\text{N}_2\text{O}_4\text{S}_2\text{Na}$ , 835.2741; found, 835.2778 ( $\text{M} + \text{Na}^+$ ).

The  $^{13}\text{C}$  NMR spectrum was shown in Fig. S2.



**Scheme S1.** Synthetic route of AU2.

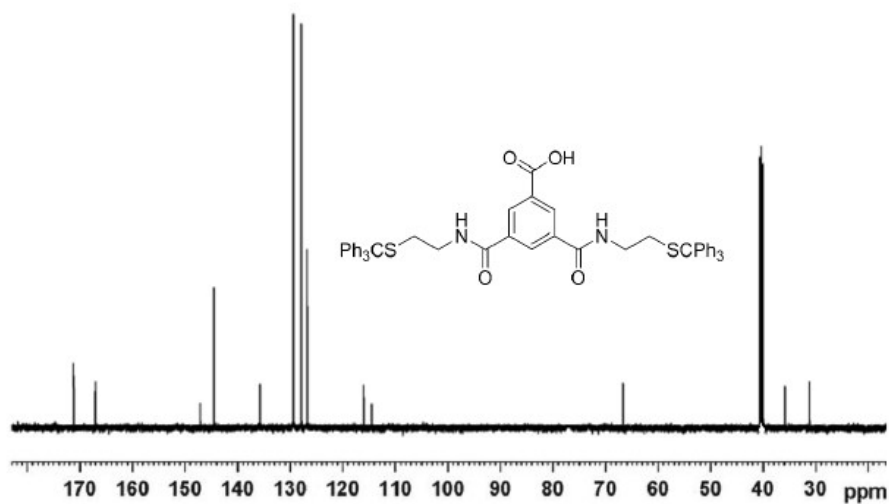


**Fig. S2.**  $^{13}\text{C}$  NMR spectrum of DL2 in  $\text{DMSO-}d_6$ .

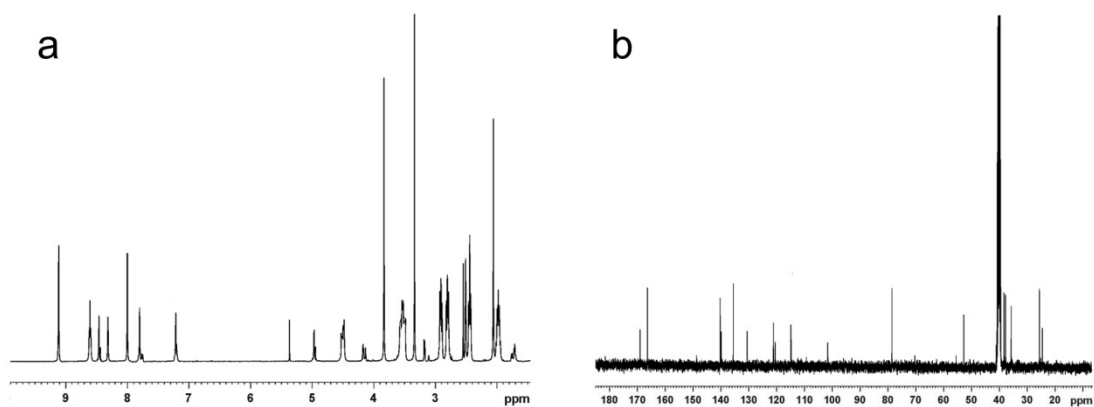


**Fig. S3.** (a)  $^1\text{H}$  NMR spectrum and (b)  $^{13}\text{C}$  NMR spectrum of Ir-DOX SMA.

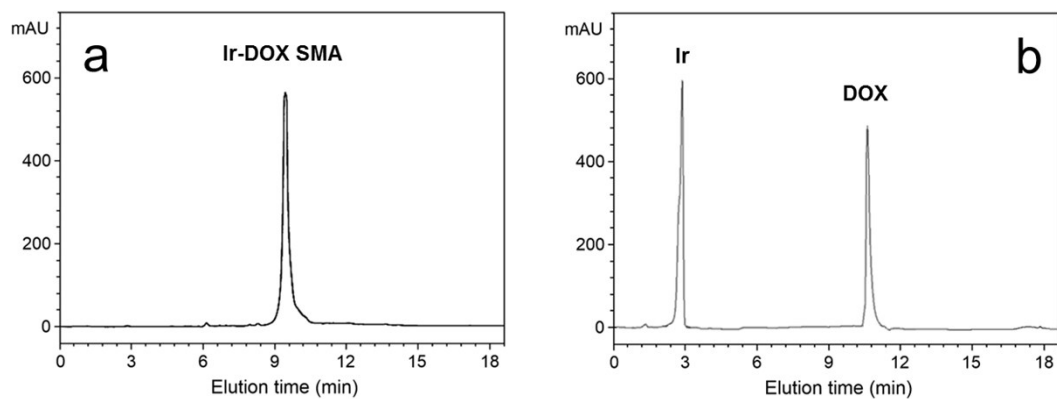


**Fig. S4.** HPLC profile of (a) Ir-DOX SMA and (b) decomposition products of Ir-DOX SMA.

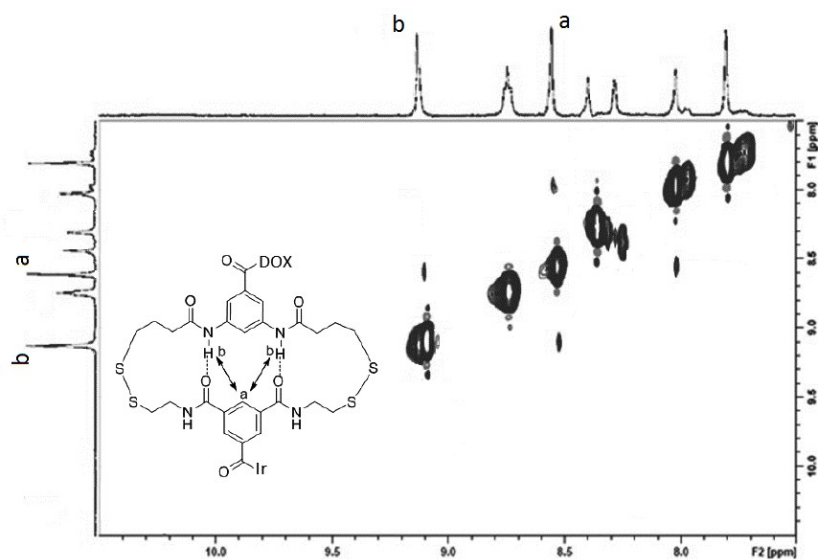


**Fig. S5.**  $^1\text{H}$ ,  $^1\text{H}$  NOSEY NMR spectra of Ir-DOX SMA.

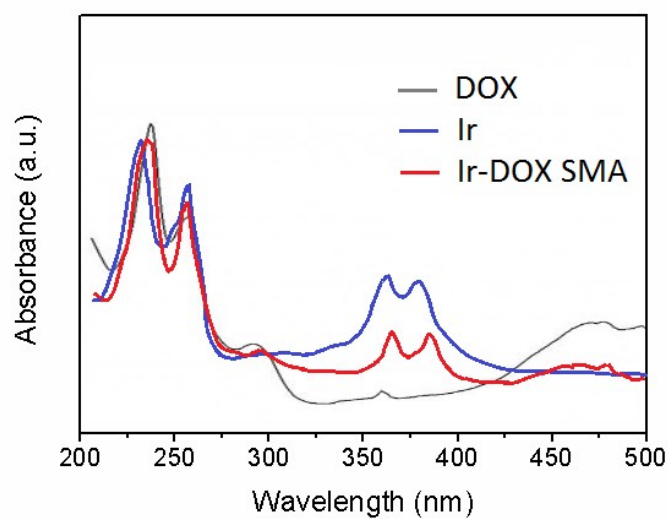


**Fig. S6.** UV-vis absorption spectra of DOX, Ir and Ir-DOX SMA.

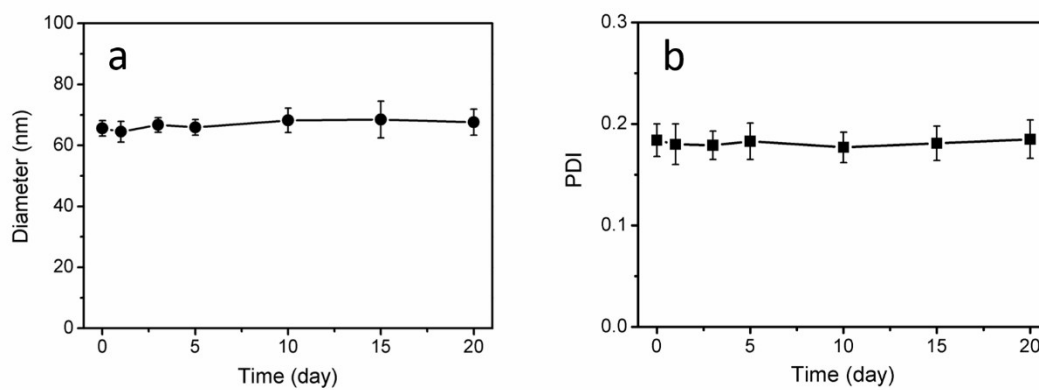


**Fig. S7.** Monitoring the changes of (a) diameter and (b) PDI of Ir-DOX SMA nanoparticles stored at 4 °C and pH 7.4 over a period of 20 days. The average size and PDI were determined at different time intervals. Data are presented as average  $\pm$  standard deviation ( $n = 3$ ).

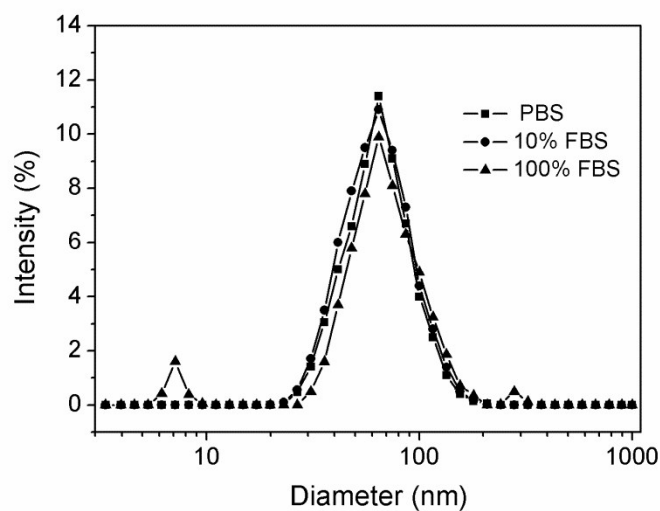


**Fig. S8.** Original size distribution of Ir-DOX SMA nanoparticles in different media based on DLS.

In the case of 100 % FBS, the protein molecules and their aggregates accounted for the small peaks at 7.3 nm and 287.2 nm, respectively. These two peaks were excluded when the average diameter and PDI were calculated.

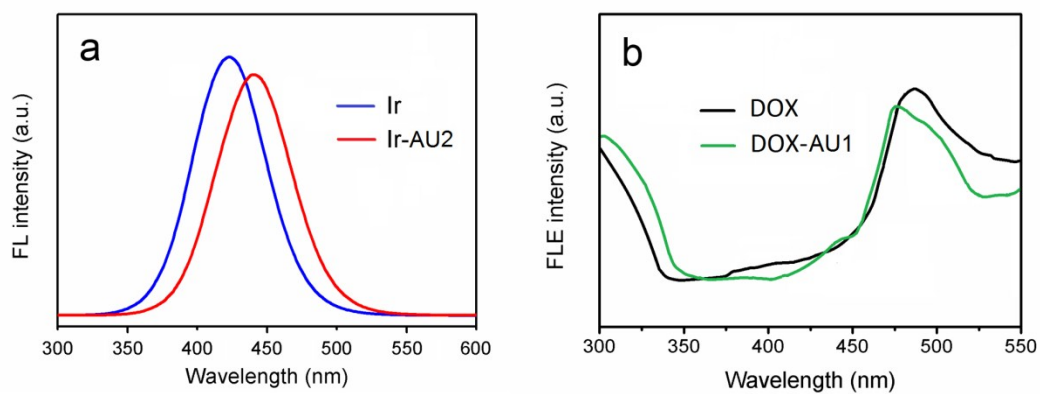


**Fig. S9.** (a) Fluorescence emission spectra of Ir and Ir-AU2. (b) Fluorescence excitation spectra of DOX and DOX-AU1.

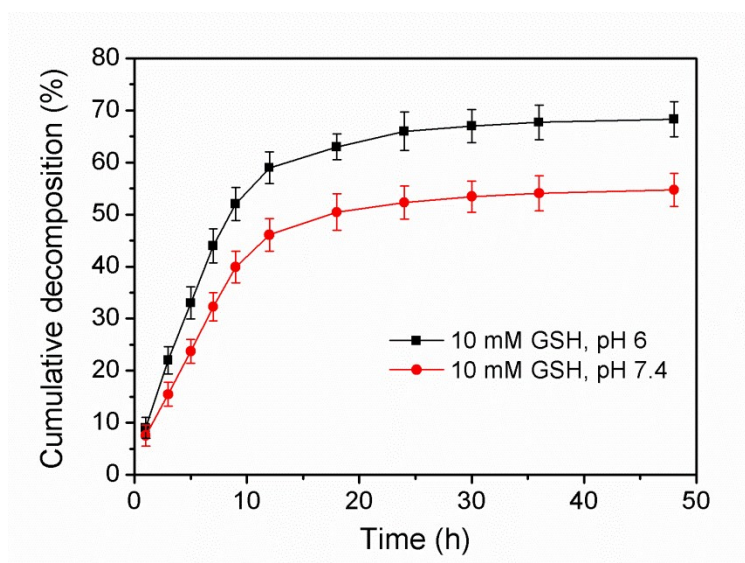


**Fig. S10.** Decomposition of Ir-DOX SMA nanoparticles in the presence of 10 mM GSH (37 °C in PBS) at pH 6 and pH 7.4, respectively, as monitored by measuring the increasing fluorescence intensity at 442 nm. Data are presented as average  $\pm$  standard deviation (n = 3).

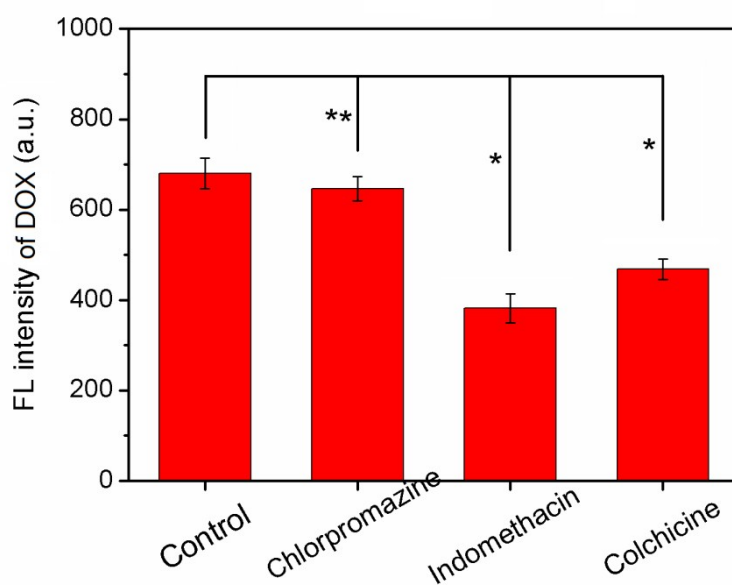


**Fig. S11.** Mechanism of cellular uptake of Ir-DOX SMA nanoparticles by CT26 cells after treatment with different endocytosis inhibitors. Data are presented as average  $\pm$  standard deviation (n = 3). Statistical significance: \*P < 0.05; \*\*P < 0.1.

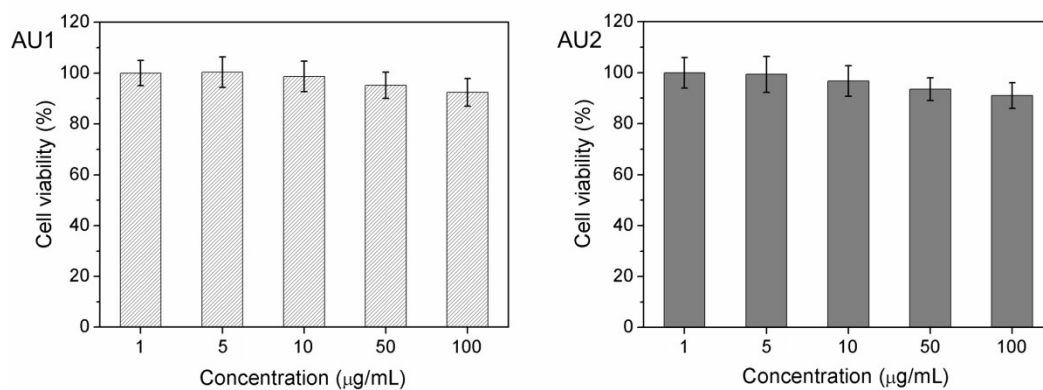


**Fig. S12.** Cytotoxicity of AU1 and AU2 to CT26 cells at varied concentrations from 1 to 100

µg/mL after incubation for 24 h.

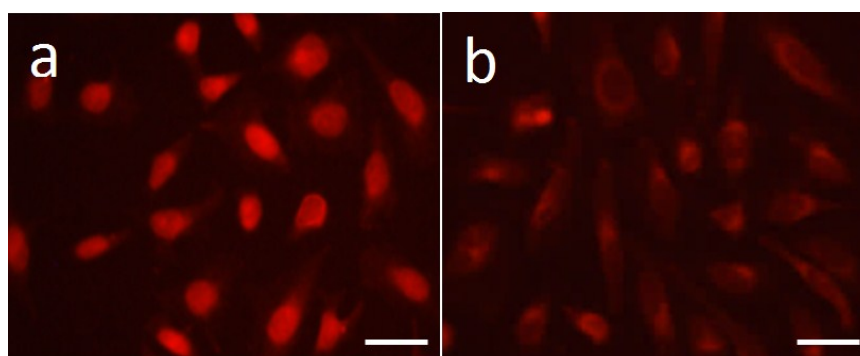


**Fig. S13.** Fluorescence images of CT26 cells incubated with Ir-DOX SMA nanoparticles for (a) 2

h and (b) 12 h at 37 °C. The scale bar in each image represents 25 µm.

#### Reference

- [1] Q. Yang, L. Bai, Y. Zhang, F. Zhu, Y. Xu, Z. Shao, Y-M. Shen, B. Gong, *Macromolecules* 47 (2014) 7431-7441.